JOURNAL OF MATERIALS SCIENCE **34** (1999) 5899–5906

Interfacial reactions between Ti-6Al-4V alloy and zirconia mold during casting

KUN-FUNG LIN, CHIEN-CHENG LIN
Department of Materials Science and Engineering, National Chiao Tung University, Hsinchu, Taiwan 300
E-mail: chienlin@cc.nctu.edu.tw

The interface of Ti-6Al-4V casting and ZrO_2 mold with silica binder was investigated by using electron probe microanalyses (EPMA), X-ray diffraction (XRD), and analytical transmission electron microscope (TEM). The interfacial reactions were proceeded by the penetration of liquid titanium through open pores near the mold surface. The metal side consisted of an α-phase layer on the top of the typical $\alpha + \beta$ two-phase substrate. In the ceramic side, zirconia was reduced by titanium to form oxygen-deficient zirconia ZrO_{2-x} and evolved a gaseous phase (presumably oxygen). The SiO_2 binder, dissolved in the ZrO_2 mold, could react with titanium to form Ti_5Si_3 in the metal side. Meanwhile, titanium could transform to titanium suboxides Ti_yO ($y \geq 2$) and the lower phase boundary of cubic ZrO_{2-x} was shifted to $ZrO_{1.76}$. Some amount of the stabilizer CaO, dissolved in Ti along with ZrO_2, could react with Ti(O) to form $Ca_3Ti_2O_7$ and $CaAl_4O_7$ in the reaction zone.

1. Introduction

Titanium alloys are widely used in the aerospace and microelectronics applications, because they have excellent properties such as high specific strength and good corrosion resistance. However, they are extremely reactive to ceramics at high temperatures, resulting in chemical reaction affected-surface [1]. The interfacial reactions between titanium and ceramics play an important role in the titanium precision casting. The interstitial elements (e.g., C, N, O, H) from the ceramic mold have a great tendency to enter into the titanium alloys during casting and cause the deterioration of mechanical properties [2]. In practice, titanium was melted in a copper crucible (water cooled) by the consumable electrode vacuum arc melting instead of vacuum induction melting (VIM) which melted titanium in a ceramic crucible. Furthermore, the casting parts of titanium alloys must be chemically milled in order to remove the reaction-affected surface.

The interfacial reactions between Ti and some dense ceramic specimens have been subjected to intensive studies. Ji *et al*. [3] showed that titanium would reduce Al_2O_3 and thus Ti_3Al precipitated in the interface of Ti and Al_2O_3 in a crucible test at 1740 °C. Koyama *et al*. [4] reported that the sputtered Ti film would react with the α-Al_2O_3 substrate, and thus formed Ti_2O, TiO, and Ti_3Al at 900 °C. In an experiment of diffusion couple, Misra [5] found that titanium reacted with α-Al_2O_3 to form TiAl and Ti_3Al at 1100 °C. Wang and Oki [6] found that titanium reacted with O from the zirconia substrate to form TiO. Ruh [7] found that zirconium entered the titanium lattice substitutionally and oxygen went to interstitial positions during the reactions between zirconia and titanium at elevated temperatures. Ruh and Garrett [8] indicated that zirconia was reduced to oxygen deficient zirconia and some zirconium existed in the grain boundary after reaction with titanium at 2000 °C/3 h.

Many researchers [9–14] have been working on the reactions of the titanium with various ceramic molds or crucibles during casting. The X-ray diffraction (XRD) analyses revealed that the reaction products of a titanium casting and the $ZrSiO_4$ mold with $Na_2Si_2O_5$ binder were TiO_2, TiO, Ti_4O_7, Ti_5Si_3, and $Na_{0.23}TiO_2$ [9]. Lyon *et al*. [10] demonstrated that a small amount of flower-like Y_2O_3 precipitated at the grain boundaries of the Ti matrix, while Y_2O_3 was reduced to Y_2O_{3-x} by judging from the darkened color of yttria. ZrO_2 was usually applied as an inert crucible or a mold face coat material in precision casting. Economos and Kingery [11] showed a considerable reaction of the zirconia crucible with titanium melt. Weber *et al*. [12] presented an unspecified feather-like eutectic phase in the reaction zone of Ti/Mg-ZrO_2. Other studies [13, 14] investigated the interfacial reactions between Ti and ceramic molds by measuring the microhardness of the alloys. The surface hardening of the titanium casting was attributed to the dissolution of oxygen that was originated from ceramic molds. However, the microhardness variation is only an indicator, not a direct observation, of the changes in the microstructure due to the interfacial reactions. While previous studies had been focused on the reactions taking place in the metal side, the transformation in the ceramic side had not been well attended.

At present study, the Ti-6Al-4V alloy was melt through a consumable electrode vacuum arc and cast

centrifugally into a porous ZrO_2 mold. After casting, thin specimens for the observation of transmission electron microscope (TEM) were prepared and the interface of titanium alloy and zirconia mold would be directly observed and characterized by an analytical TEM. The microstructural characterization was also aided by scanning electron microscopy (SEM), X-ray diffraction (XRD), and electron probe microanalyses (EPMA). Finally, we would attempt to elucidate the mechanism of the interfacial reactions between titanium and zirconia mold during casting.

2. Experimental procedures

The experimental procedures were displayed by the flow chart in Fig. 1. The wax patterns were prepared by injecting wax into a metal die, and then assembled into a wax tree. The wax tree was then dipped in the primary ceramic slurry which was mixed from 80 wt % fine zirconia filler (325 mesh, 4%CaO partial stabilized ZrO_2), 20 wt % colloidal silica (15 nm, 30% SiO_2), a wetting agent (Vitawet 12), and an antifoaming agent. It was then stuccoed with coarse zirconia particles (100 mesh, 98%ZrO_2) after draining the excess slurry. The mold was dried in air at a properly controlled temperature (22–24 °C) and 50% relative humidity. These processes were repeated twice and thus the so-called face coats were obtained. On the top of face coats, the mold was built up to 10 mm in thickness by alternating with mullite slurry and stucco. The mold was dewaxed in an autoclave at 8 bar for 12 min after final drying over 24 h, and then sintered at 1050 °C for 2 h. It was set up at a centrifugal table and preheated at 350 °C for 1 h. A Ti-6Al-4V electrode was melt and cast into the zirconia mold with 300 rpm in the consumable electrode vacuum arc furnace at 10^{-2} torr.

As-cast specimens were analyzed by TEM (JOEL JEM 2010) as well as SEM (JXA-6400), XRD (Rigaku D), and EPMA (JXA-8621MX). Cross-sectional TEM specimens perpendicular to the interface of ceramics and metal were prepared by standard procedures of cutting, grinding, polishing, and ion milling. The quantitative composition analyses were carried out based on the principle of Cliffs-Lorimer method by an energy dispersive spectroscope (EDS, D-Link) attached to the TEM.

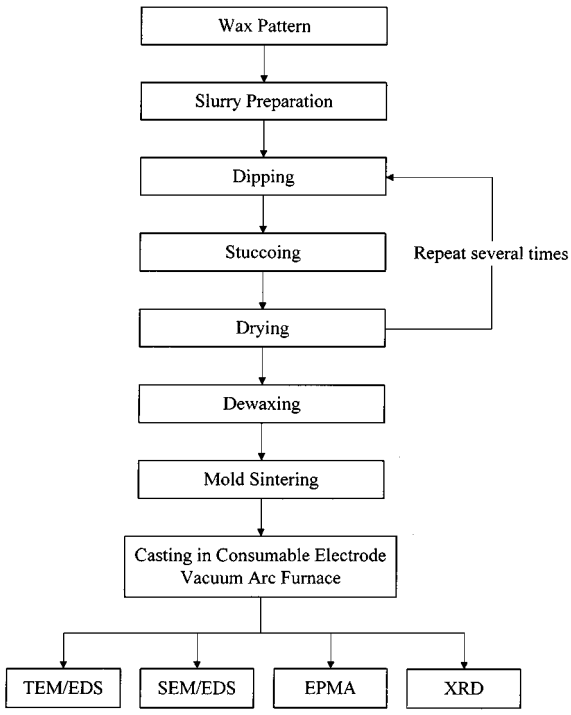

Figure 1 The flow chart of experimental procedures.

3. Results

An SEM micrograph of the as-sintered ceramic mold is shown in Fig. 2a. The large angular particles (about 90 μm) are ZrO_2 stucco, while the smaller particles ($\approx$30 μm) are ZrO_2 fillers. The as-sintered mold displays a porous structure with fine particles dispersed near the mold surface. The EDS of finer ceramic particles at the face coat is shown in Fig. 2b, indicating that the silica binder could be dissolved into the calcia-partially-stabilized ZrO_2 during sintering.

Fig. 3a is an SEM micrograph showing the interface of a thin ($\approx$2 mm thick) Ti-6Al-4V and the zirconia mold. In the right of this micrograph, there exists a two phase ($\alpha + \beta$) region, a typical structure of the commercial Ti-6Al-4V alloy. The α-phase is located at the center of the micrograph, the zirconia mold in the left of the micrograph. EPMA results indicated that in addition to Ti, Al, and V, the α-phase contained O and Zr which came from the zirconia mold. During casting, the liquid titanium infiltrated into the zirconia mold through the open pores in the mold surface by both capillary and centrifugal forces. ZrO_2 particles surrounded by the molten alloy were gradually dissolved with the formation of small bubbles in the α-phase. Fig. 3b is the concentration profile of oxygen, indicating a diffusion depth of about 100 μm in the casting. The oxygen was rich in the α-case layer, resulting in hardening at the surface of the casts.

The oxygen atom is a stabilizer of α-phase, while zirconium is a stabilizer of β-phase [15]. Both of two stabilizing elements could affect the microstructure of the as-cast specimens. Since the diffusivity of oxygen in α-Ti is much faster than that of zirconium [14] and titanium has a great affinity with oxygen, a single α-Ti(O) layer was thus formed at the interface, leaving a solid solution of ZrO_{2-x} behind in the ceramic mold. This is consistent with the results reported by Saha *et al.* [16]. This layer of α-Ti(O) was the so-called α-case, which was very hard and brittle due to oxygen interstitial effects [17]. There also existed some cracks in the α-case. It was easily delaminated due to the collapse of shell mold, blast off, and cut off after cast. The reaction layer appeared as a dark gray color, an indication of the formation of oxygen deficit zirconia [18, 19].

The chipped off reaction layer was powdered and investigated by XRD. The XRD spectrum in Fig. 4 indicates the formation of Ti_2O phase after reaction. Ti_2O is a solid solution of α-Ti(O) with an ordered structure at low temperatures. Since the solubility of oxygen in titanium at high temperatures is higher than that at low temperatures, the oxygen would precipitate during solidification.

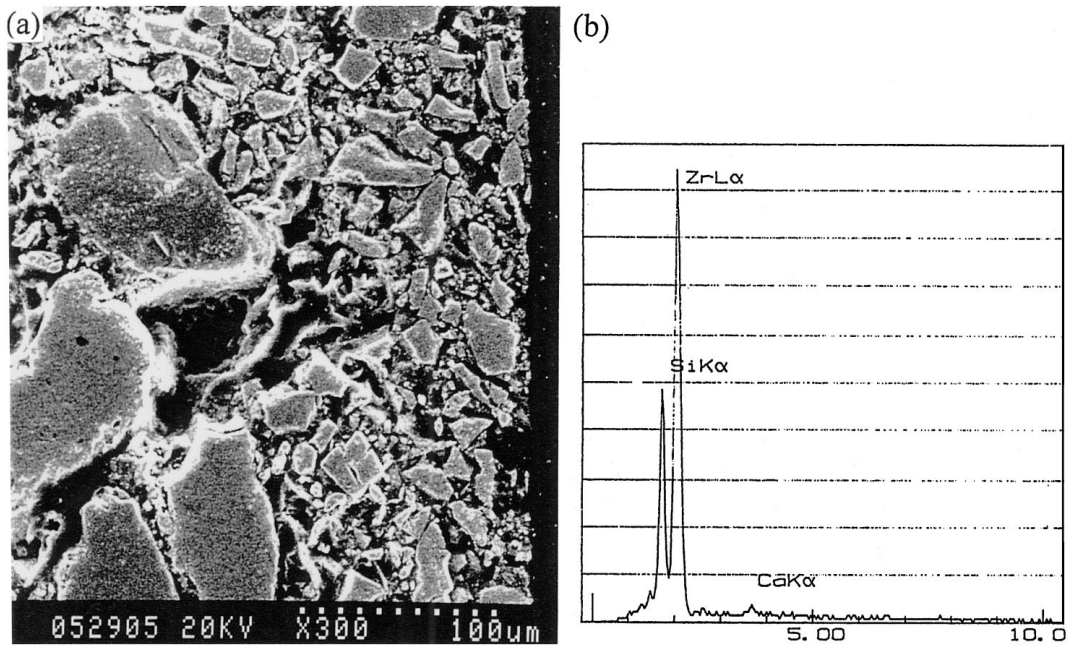

Figure 2 (a) An SEM micrograph of the as-sintered ceramic mold showing a porous structure; (b) An EDS indicates that the silica binder was dissolved into fine zirconia particles at the face coat.

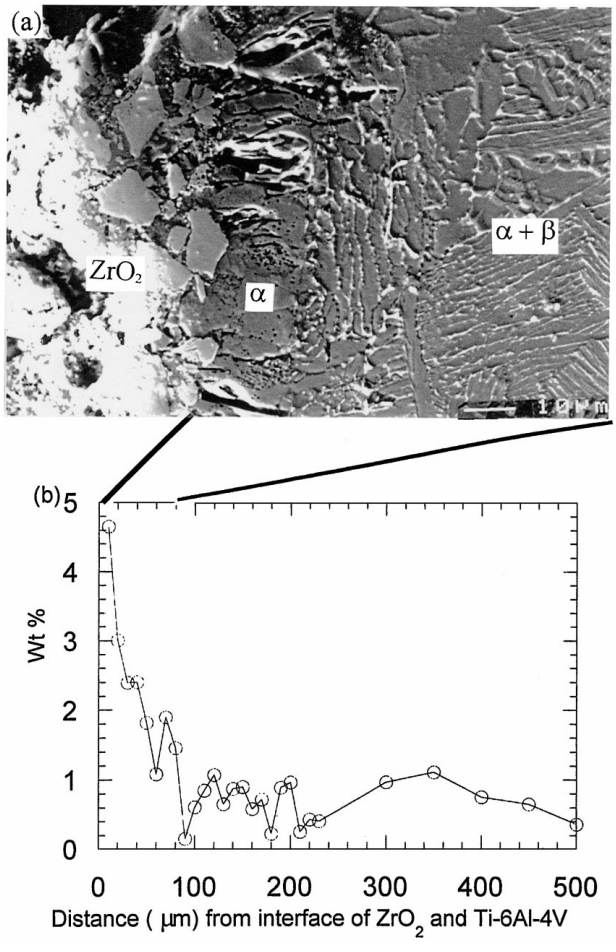

Figure 3 (a) An SEM micrograph showing the reaction zone of a thin (≈2 mm) Ti-6Al-4V and the ZrO_2 mold; (b) An oxygen concentration profile. The lines connecting (a) and (b) indicate the corresponding depths.

Fig. 5a shows a SEM micrograph of the reaction layer of a thick (≈70 mm) Ti-6Al-4V and the zirconia mold. The distributions of Ti, Si, O, Ca, and Zr elements in the reaction layer were demonstrated by X-ray mappings in Fig. 5b–f, respectively. The phase designated as "A" in Fig. 5a is α-Ti(O) which dissolved some Zr and O. The fact that a compound of Ti-Si, designated as "B" in Fig. 5a, was formed during casting indicates that silica in the ceramic mold could react with titanium. The fine zirconia particles with pores, designated as "C" in Fig. 5a, were embedded in the metal and their surfaces became irregular after being severely dissolved by titanium. The fine zirconia was rich of Ca and Zr elements as shown in Fig. 5e and f. During casting, a significant amount of oxygen was leached from zirconia by titanium. While part of these leached oxygen was accumulated as bubbles, the remaining was dissolved in the melt, which could precipitate from supersaturated α-Ti(O) during solidification.

Fig. 6a is a bright field image of α-Ti(O) and ZrO_{2-x} in the reaction layer. The EDS in Fig. 6b demonstrated that the α-Ti(O) contained 7.89 at % O as well as a small amount of zirconium element (1.84 at % Zr). On the other hand, the zirconia mold was reduced by titanium into an oxygen deficient zirconia with O/Zr ratio being 1.76 (Fig. 6c). The EDS result also indicates that this oxygen deficit zirconia dissolved a small amount of Ti (≈2.58 at %).

As mentioned in Fig. 2, the silica binder could be dissolved in the zirconia mold. During casting, the silica along with zirconia was dissolved into titanium. Since the solubility of Si in α-Ti was limited at low temperature [20], the Ti-Si compound precipitated on cooling, leaving a limited Si in the α-Ti (Fig. 6b). Fig. 7a and b are the bright field image and dark field image of a titanium silicide compound in the titanium, respectively. The titanium silicide compound is identified to be hexagonal Ti_5Si_3 from its SADP (Fig. 7c). The EDS result, as shown in Fig. 7d, reveals that Ti_5Si_3 dissolved 6.10 at % Al, 4.31 at % V, and 7.61 at % Zr.

Fig. 8a and 8b are the bright field image and the selected area diffraction pattern (SADP), respectively, of Ti_3O that was found in the reaction layer. The

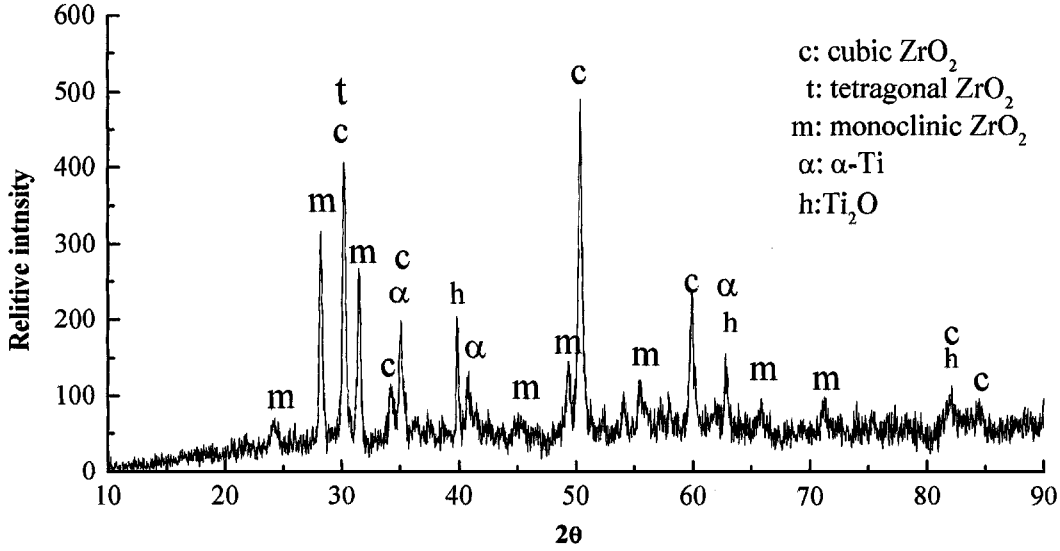

Figure 4 An XRD spectrum of the reaction layer of a thick (≈70 mm) Ti-6Al-4V and the ZrO_2 mold after slow cooling.

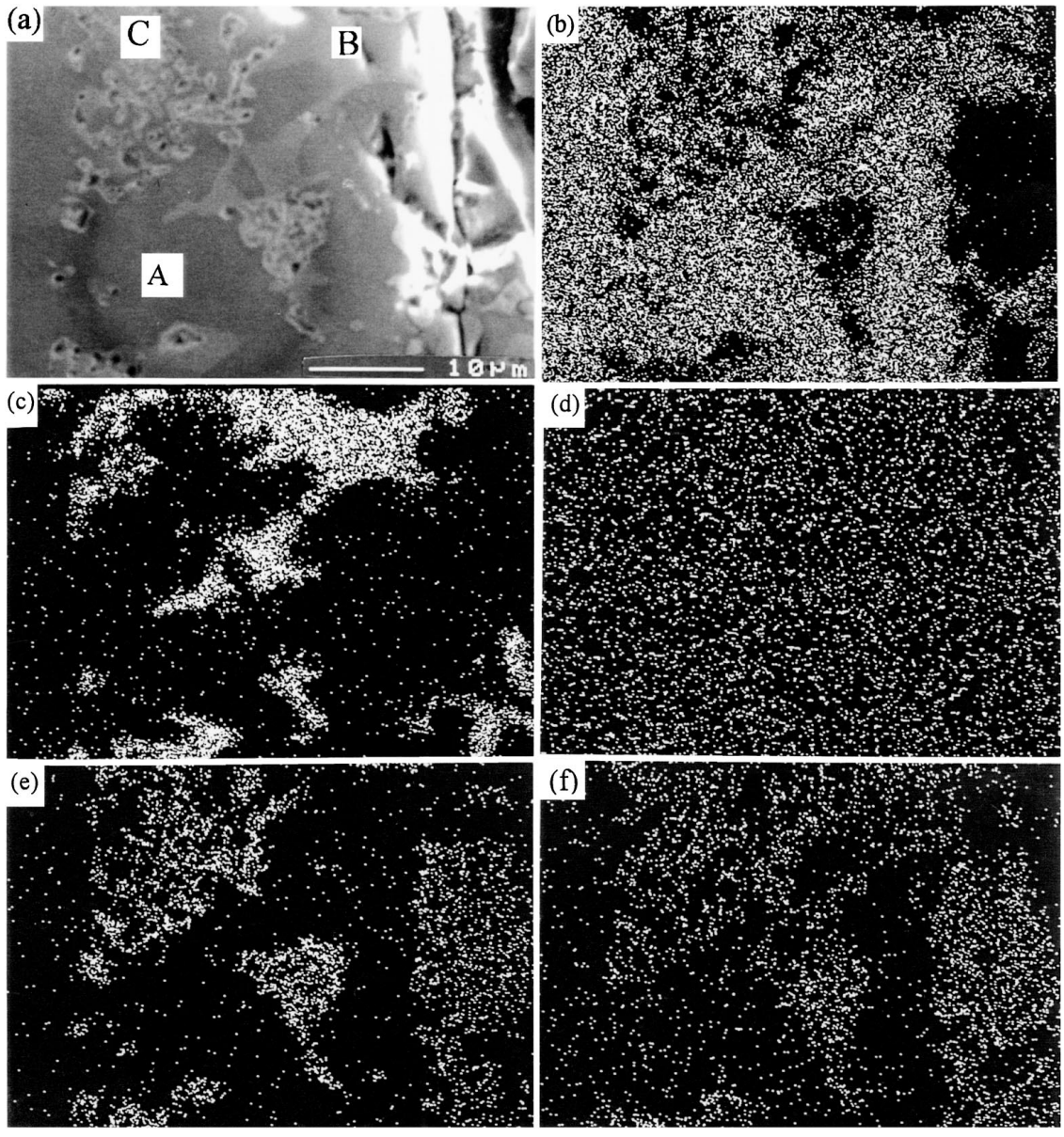

Figure 5 (a) An SEM micrograph showing the reaction layer of a thick (≈70 mm) Ti-6Al-4V and the ZrO_2 mold after slow cooling; the X-ray mappings, respectively, of (b) Ti; (c) Si; (d) O; (e) Ca; (f) Zr.

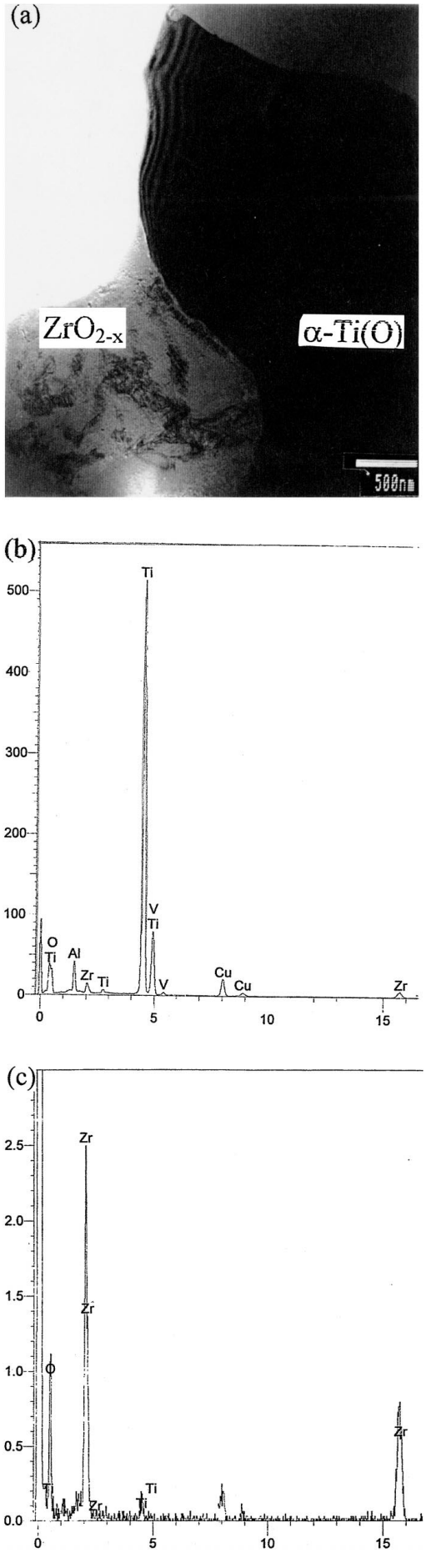

Figure 6 (a) A TEM micrograph showing α-Ti(O) and ZrO_{2-x}; (b) EDS of α-Ti(O); (c) EDS of ZrO_{2-x}.

superlattice reflections (00·1), (00·2), (11·1), and (11·2) indicate that this phase is an ordered structure of Ti_3O. The superlatice reflections of (00·2) belonged to the type I ($h = 3n$, $k = 3n$, $l = 8n' + 2$, $l = 8n' + 6$) [21]. However, other superlatice reflections (hk·1) such as (00·1) (11·1) (11·2), where $h - k = 3n$, $l \neq 3n$, showed a discrepancy with the type I. The reflection (00·1) was observed by Andersson *et al*. [22], while the reflection (11·2) might be caused by the displacement of titanium from the ideal position of the h.c.p. lattice [21]. Since the reflection of (11·1) was forbidden from the calculation of structure factor [21], its appearance could be caused by double diffraction.

There also existed $Ca_3Ti_2O_7$ and $CaAl_4O_7$ in the reaction layer. The bright field image and SADP of $Ca_3Ti_2O_7$ are displayed in Fig. 9a and 9b respectively, while those of $CaAl_4O_7$ are in Fig. 9c and 9d. This result indicated that the CaO stabilizer was extensively dissolved along with ZrO_2 into titanium during reaction, causing the formation of $Ca_3Ti_2O_7$ and $CaAl_4O_7$.

4. Discussions

(1) Thermodynamics consideration

The following interfacial reactions between Ti and ZrO_2 are not thermodynamic favorable, because the Gibbs free energies of following equations are positive or slightly negative at 1727 °C [23].

$$Ti + ZrO_2 \rightarrow TiO + Zr + 1/2\ O_2$$
$$\Delta G_1^\circ = 157.15\ \text{kcal/mol}$$
$$Ti + ZrO_2 \rightarrow TiO_2 + Zr$$
$$\Delta G_2^\circ = 33.14\ \text{kcal/mol}$$
$$2Ti + 3/2\ ZrO_2 \rightarrow Ti_2O_3 + 3/2\ Zr$$
$$\Delta G_3^\circ = -0.42\ \text{kcal/mol}$$
$$3Ti + 5/2\ ZrO_2 \rightarrow Ti_3O_5 + 5/2\ Zr$$
$$\Delta G_4^\circ = 26.82\ \text{kcal/mol}$$

It is inferred titanium can not be a reducing agent for zirconia. However, it was found in this study that ZrO_2 was transformed to ZrO_{2-x} and some gaseous phase was evolved. Domagala *et al*. [24] indicated that more than 20 at % of ZrO_2 could be dissolved in Ti at high temperatures. Lyon *et al*. [10] stated that the formation energy of Ti-10 at % O solution at 1400 °C was more negative than that of ZrO_2. In the present study, Ti reduce the zirconia at high temperatures. The existence of the titanium sub-oxides (Ti_2O, Ti_3O) and oxygen-deficient zirconia (ZrO_{2-x}) showed that the zirconia was partially reduced by titanium during solidification. It implied that the interfacial reactions between titanium alloy and zirconia could not be predicted solely by thermodynamic calculation of the formation energy difference between titanium oxide and zirconia, because the activity of Ti in solid solution was unknown in this complex system.

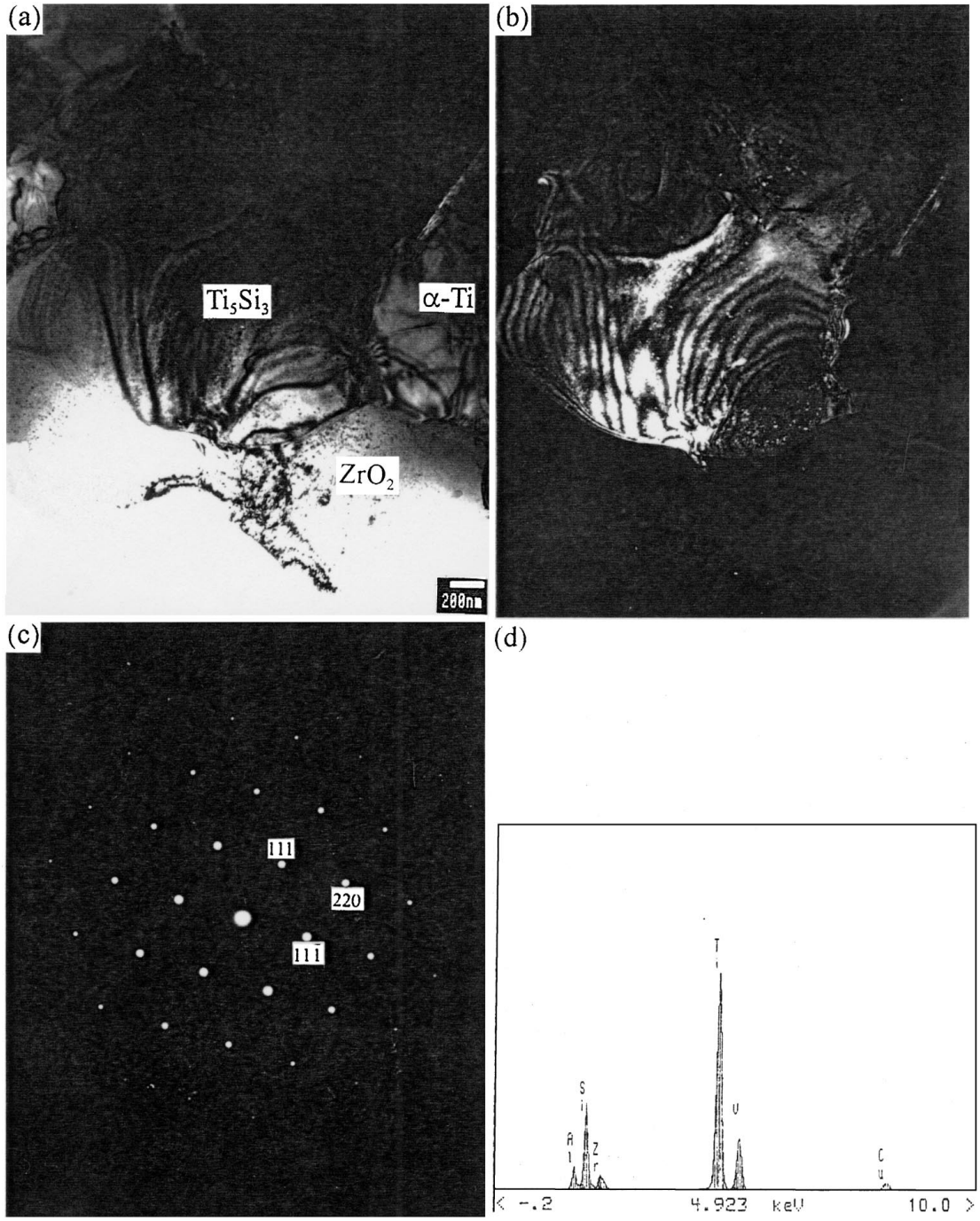

Figure 7 (a) The bright field image of Ti_5Si_3 in Ti6Al4V; (b) The dark field image of the Ti_5Si_3; (c) SADP, $Z = [1\,\bar{1}\,0]$; (d) EDS of Ti_5Si_3.

(2) Ti → Ti_xO transition

Titanium reacted with zirconia and transformed to α-Ti(O) solid solution as a result of precision casting. The Ti-O phase diagram shows O has a large solubility in α-Ti at high temperatures, and some titanium sub-oxides exist at low temperatures. The ordered cph phases, Ti_2O, Ti_3O and possibly Ti_6O, are formed within an extended range [25]. Present results displayed that the ordered titanium suboxides Ti_3O and Ti_2O were found in the reaction layer, in addition that a significant amount of oxygen was dissolved in the surface of titanium. Accompanying the α-phase in the reaction layer were many gas bubbles. It indicated that the titanium suboxides could form via an order and disorder transformation. Since Ti_2O was more stable than TiO [26], the ordered titanium suboxides formed in the reaction layer was Ti_2O rather than TiO.

(3) ZrO_2 → ZrO_{2-x} transition

ZrO_2 was reduced to ZrO_{2-x} and dissolved some α-Ti(O) during precision casting. The composition of cubic ZrO_{2-x} in the reaction layers was approximated to be $ZrO_{1.76}$. The Zr-O system, particularly the ZrO_2 rich portions, shows a broad range of O loss down to 1200 °C owing to thermal effects. Such a loss significantly lowers the cubic-tetragonal phase transformation temperature from 2400–1500 °C at 13% O loss, and may have a similar effect on the monoclinic-tetragonal transformation [27]. From the lower phase boundary of ZrO_{2-x} at high temperatures (1956–2404 °C), the oxygen contents extends from 63.5 at % to 60.8 at %, or $1.55 < O/Zr < 1.74$, respectively [28]. However, the O/Zr ratio for ZrO_{2-x} at 1300 °C is between 1.925 and 2.0 [29].

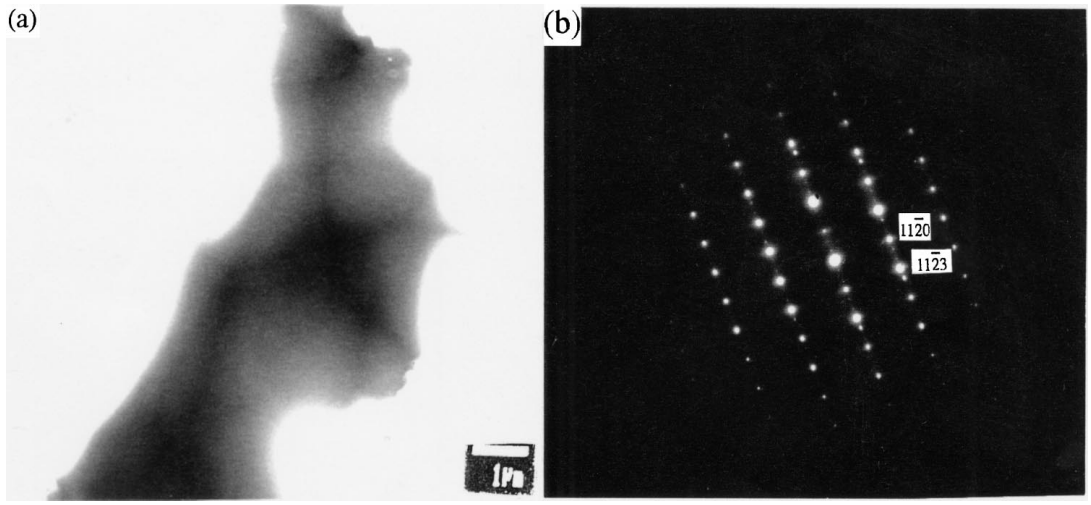

Figure 8 The Ti_3O phase with an ordered structure was found in the reaction layer: (a) The bright field image; (b) SADP, $Z = [\bar{1}\,100]$.

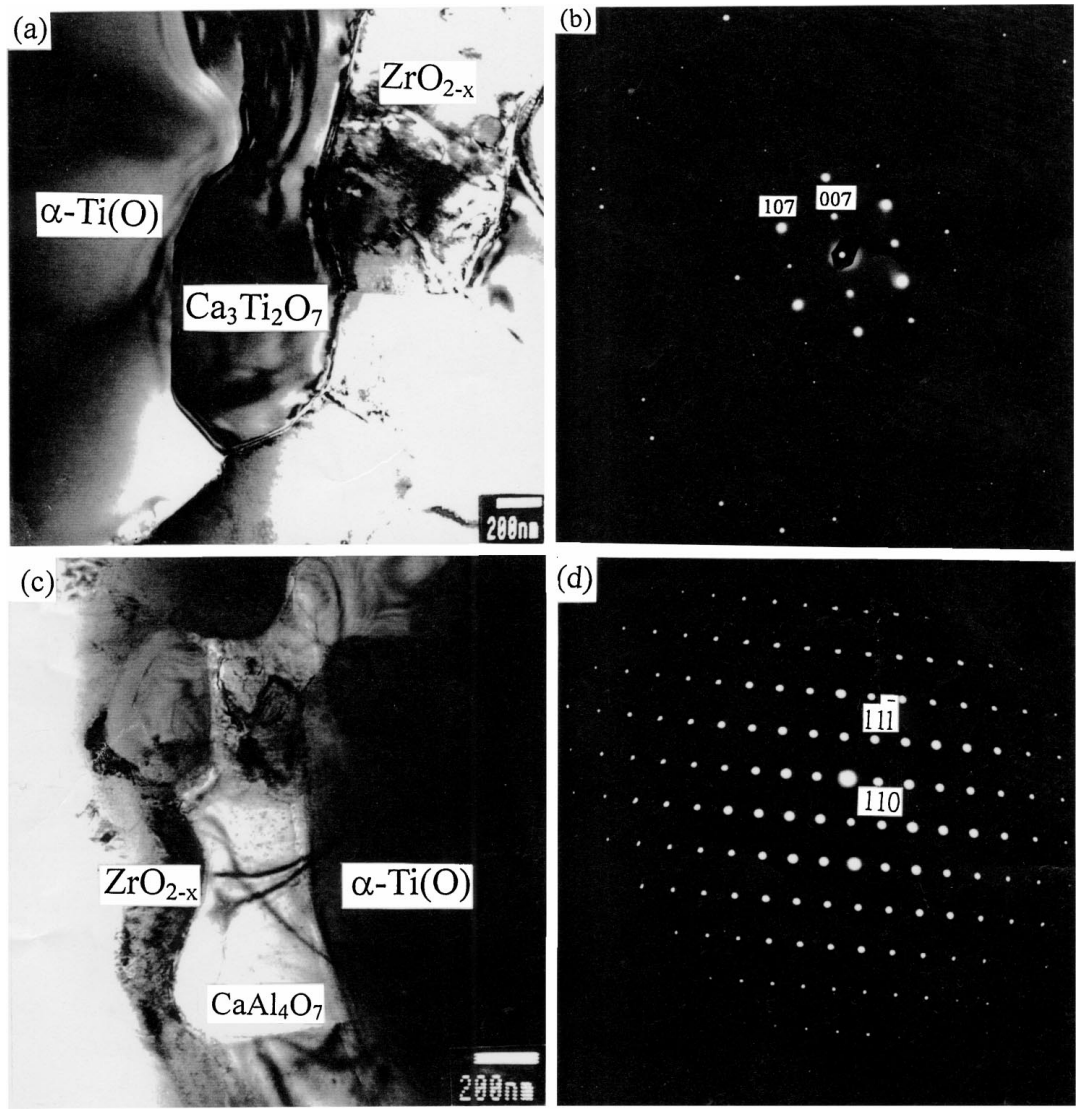

Figure 9 The existence of $Ca_3Ti_2O_7$ and $CaAl_4O_7$ in the reaction layer: (a) The bright field of $Ca_3Ti_2O_7$; (b) The SADP of $Ca_3Ti_2O_7$, $Z = [0\,\bar{1}\,0]$; (c) The bright field image of $CaAl_4O_7$; (d) The SADP of $CaAl_4O_7$, $Z = [\bar{1}\,1\,0]$.

In the reaction layer, the titanium was transformed to α-Ti(O) and the ordered titanium suboxides Ti_yO formed at low temperatures. The dissolution of Ti(O) in ZrO_{2-x} (Fig. 6(c)) could induce a large concentration of point defects ionized oxygen vacancy and cation interstitial due to the valence effects, causing the variation of the lattice structure. The oxygen vacancy associated with Zr could provide stabilization for tetragonal and cubic zirconia [30]. It is believed that the substitution of titanium ion for Zr^{+4} could retard the

transformation of cubic oxygen deficient zirconia, even though CaO was expelled from some ZrO_2 (Fig. 9).

(4) Mechanism of interfacial reactions

The interfacial reactions between Ti-6Al-4V and ZrO_2 can be summarized as follows. During casting, the liquid titanium penetrated into the ceramic mold through the interconnected pores near the mold surface, and thus zirconia particles were embedded in the Ti melt. Titanium would dissolute zirconia and then the surface of ZrO_2 was gradually rounded. Interdiffusion of Zr, O and Ti took place at the interface and the solid solution of ZrO_2 in Ti(O) was formed at high temperatures. Subsequently, ZrO_2 was reduced into ZrO_{2-x} and oxygen was evolved at high temperatures. Part of the oxygen was accumulated as bubbles, while the remaining was dissolved in the melt that could precipitate from supersaturated α-Ti(O) during solidification. Meanwhile, α-Ti(O) transformed to Ti_yO ordered structures such as Ti_2O and Ti_3O during cooling. The titanium could also react with CaO, the stabilizer of ZrO_2, giving rise to the formation of the compounds $Ca_3Ti_2O_7$ and/or $CaAl_4O_7$.

5. Conclusions

1. Interfacial reactions between Ti-6Al-4V and ZrO_2 mold during casting were proceeded by the penetration of liquid titanium due to capillary and centrifugal forces through the interconnected pores near the mold surface. Ti reduced ZrO_2 and leached oxygen to form the α-Ti(O) solid solution, which could exist as the ordered structure of Ti_yO ($y \geq 2$) at low temperatures. The solid solution of Zr in α-Ti(O) was also found.

2. ZrO_2 was reduced to c-ZrO_{2-x} by titanium and oxygen was simultaneously evolved during casting. Part of the evolved oxygen from zirconia was accumulated as bubbles at high temperatures, while the remaining was dissolved in melt that could precipitate during solidification.

3. The SiO_2 binder in ZrO_2 mold would react with titanium to form Ti_5Si_3 in the titanium. Some amount of the stabilizer CaO, dissolved in Ti along with ZrO_2, could react with Ti(O) to form $Ca_3Ti_2O_7$ and $CaAl_4O_7$ in the reaction zone.

Acknowledgements

This research was sponsored by the National Science Council, Taiwan, under the Contract No. NSC 87-2216-E009-014.

References

1. R. L. SAHA and K. T. JACOB, *Def. Sci. J.* **36**(2) (1986) 121–141.
2. M. J. DONACHIE, JR. "Titanium: A Technical Guide" (ASM International, Metals Park, Ohio, 1988) p. 40.
3. H. JI, S. JONES and P. M. MARQUIS, *J. Mater. Sci.* **30** (1995) 5617–5620.
4. M. KOYAMA, S. ARAI, S. SUENAGA and M. NAKAHASHI, *ibid.* **28** (1993) 830–834.
5. A. K. MISRA, *Metall. Trans.* **22A** (1991) 715–721.
6. L. D. WANG and T. OKI, *J. Ceram. Soc. Japan.* **103**(7) (1995) 671–674.
7. R. RUH, *ibid.* **46**(7) (1963) 301–306.
8. R. RUH and H. J. GARRETT, *ibid.* **50**(5) (1967) 257–261.
9. R. L. SAHA and R. D. K. MISRA, *J. Mater. Sci. Lett.* **10** (1991) 1318–1319.
10. S. R. LYON, S. INOUYE, C. A. ALEXANDER and D. E. NIESZ, in Fourth World Conference of Titanium, Japan, 1980, pp. 271–284.
11. G. ECONOMOS and W. D. KINGERY, *J. Am. Ceram. Soc.* **36**(12) (1953) 403–409.
12. B. C. WEBER, W. M. THOMPSON, H. O. BIELSTEIN and M. A. SCHWARTZ, *J. Am. Ceram. Soc.* **40**(11) (1957) 363–373.
13. K. I. SUZUKI, S. WATAKABE and K. NISHIKAWA, *J. Japan. Inst.* **60**(8) (1996) 734–743.
14. R. L. SAHA, T. K. NANDY, R. D. K. MISRA and K. T. JACOB, *Bull. Mater. Sci.* **12**(5) (1989) 481–493.
15. J. L. WAKTER, M. R. JACKSON and C. T. SIMS "Alloying" (ASM International, Metals Park, Ohio, 1988) p. 258.
16. R. L. SAHA, T. K. NANDY, R. D. K. MISRA and K. T. JACOB, *Metall. Trans.* **21B**(6) (1990) 559–566.
17. A. I. KAHVECI and G. E. WELSCH, *Scripta. Metall.* **20** (1986) 1287–1290.
18. R. RUH, N. M. TALLAN and H. A. LIPSITT, *J. Am. Ceram. Soc.* **47**(12) (1964) 632–635.
19. J. S. MOYA, R. MORENO and J. REQUENA, *ibid.* **71**(11) (1988) 479–480.
20. J. L. MURRY in "Phase Diagrams of Binary Titanium alloy" (ASM International, Metal Park, Ohio, 1987) p. 289.
21. S. YAMAGUCHI, *J. of Phy. Soc. Japan.* **27**(1) July (1969) 155–163.
22. S. ANDERSSON, B. COLLEN, U. KUYKENSTIERNA and A. MAGNELI, *Acta Chem. Scand.* **11**(10) (1957) 1641–1652.
23. U.S. Department of Commerce, JANAF thermochemical tables, National Bureau of Standards, U.S. Department of Commerce, Michigan, 1971.
24. R. F. DOMAGALA, S. R. LYON and R. RUH, *J. Am. Ceram. Soc.* **56**(11) (1973) 584–587.
25. J. L. MURRY in "Phase Diagrams of Binary Titanium alloy" (ASM International, Metal Park, Ohio, 1987) p. 211.
26. J. J. PAK, M. L. SANTELLA and R. J. FRUEHAN, *Metall. Trans.* **21B**(4) (1990) 349–355.
27. R. W. RICE, *J. Am. Ceram. Soc.* **74**(7) (1991) 1745–1746.
28. R. J. ACKERMANN, S. P. GARG and E. G. RAUH, *ibid.* **60**(7–8) (1977) 341–345.
29. *Idem.*, *ibid.* **61**(5–6) (1978) 275–276.
30. P. LI, I. W. CHEN and J. E. PENNER-HAHN, *ibid.* **77**(1) (1994) 118–128.

Received 23 December 1997
and accepted 27 April 1999